Simultaneous, noninvasive observation of elastic scattering, fluorescence and inelastic scattering as a monitor of blood flow and hematocrit in human fingertip capillary beds

Joseph Chaiken,[a,*] Jerry Goodisman,[a] Bin Deng,[a] Rebecca J. Bussjager,[b] and George Shaheen[b]

[a]Syracuse University, CST1-014, Department of Chemistry and Department of Chemical and Biomedical Engineering, Syracuse, New York 13244-4100

[b]LightTouch Medical, Inc., 600 East Genesee Street, Suite 123, Syracuse, New York 13201

Abstract. We report simultaneous observation of elastic scattering, fluorescence, and inelastic scattering from *in vivo* near-infrared probing of human skin. Careful control of the mechanical force needed to obtain reliable registration of *in vivo* tissue with an appropriate optical system allows reproducible observation of blood flow in capillary beds of human volar side fingertips. The time dependence of the elastically scattered light is highly correlated with that of the combined fluorescence and Raman scattered light. We interpret this in terms of turbidity (the impeding effect of red blood cells on optical propagation to and from the scattering centers) and the changes in the volume percentages of the tissues in the irradiated volume with normal homeostatic processes. By fitting to a model, these measurements may be used to determine volume fractions of plasma and RBCs. [DOI: 10.1117/1.3233629]

Keywords: Raman; fluorescence; glucose; noninvasive; blood analysis; hematocrit.

Paper 09203LR received May 20, 2009; revised manuscript received Jul. 19, 2009; accepted for publication Aug. 5, 2009; published online Oct. 7, 2009.

1 Introduction

There is considerable interest[1] in spectroscopic probing of tissue *in vivo* noninvasively. We are interested in blood analysis for glucose[2,3] and other analytes (e.g., bicarbonate, hematocrit). We have developed apparatus[4] that allows accurate and reproducible registration of human volar side fingertips with a near-infrared (NIR) laser Raman spectroscopic system. By "registration," we include control of the pressure between the skin surface and the aperture or template defining the entrance into the optical collection system. This pressure and the shape of the aperture affect the flow of blood [i.e., plasma and red blood cells (RBCs) in the capillaries]. We report observations pertinent to obtaining separate and simultaneous measures of plasma and RBC content in the fingertip capillaries.

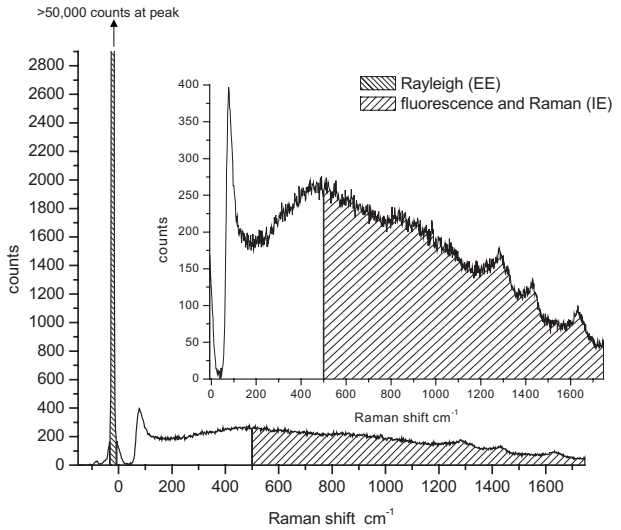

Fig. 1 Top: Raw typical single 20 ms frame of Andor CCD output with system optimally aligned using 200 mW of 830 nm excitation. Bottom: Sections of emission used to calculate IE ($\approx$500–1750 cm^{-1}) and EE (−30 to +10 cm^{-1}).

The optical properties of the tissues[5–7] for 830 nm incident light are (μ_a=0.03 mm^{-1}, μ_s=0.06 mm^{-1}) for plasma, (0.45, 30.0) for RBCs, and (0.5, 1.2) for static tissue. Despite the very low volume fraction[8–10] of RBCs (i.e., 0.005–0.003), the optical constants of plasma, red blood cells, and other skin constituent materials are such that the net propagation of light is mostly determined by the RBCs. Skin (i.e., "static tissue" that does not move when pressed but instead deforms) has a tenfold larger scattering coefficient than plasma. That of RBCs exceeds that of skin by *at least* a factor of 20.

The inelastic light originates from fluorescence and Raman scattering. The fluorescence is stronger, and there are overlapping components from all tissues in the irradiated volume (i.e., plasma, RBCs, and skin). The fluorescence yield per unit volume is different for plasma, RBCs, and skin. Because they result from fundamentally different physical processes, the apparent fluorescence (and Raman) yields differ between RBCs, plasma, and skin in a manner that is uncorrelated with the variation in elastic scattering yields across the same tissues. A model that takes these parameters into account should allow us to simultaneously estimate the volume fractions of these tissues, *in vivo* and noninvasively.

2 Experimental

The experimental apparatus and many experimental details have been previously published.[2,3,11] The top of Fig. 1 shows a raw typical single frame of Andor CCD output and the bottom shows the same frame on an expanded scale to show the sections of emission integrated to obtain combined fluorescence and Raman emission; hereafter referred to as "inelastic emission" (IE) and elastic emission (EE). The IE spectral region was chosen to exclude as much as possible of the Rayleigh line and off-axis reflected light from the outermost stra-

*Tel: 315-443-4285; E-mail: jchaiken@syr.edu

1083-3668/2009/14(5)/050505/3/$25.00 © 2009 SPIE

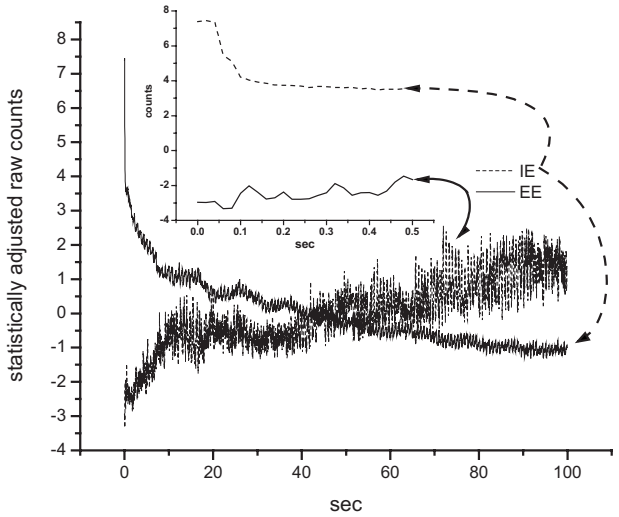

Fig. 2 Integrated inelastic scattered light + fluorescence and integrated elastic scattered light as a function of time for a single very short and weak mechanical impulse; starting at time $t=0$ s, followed by active pressure maintenance at 50 g/cm^2. Inset: same data at shortest times.

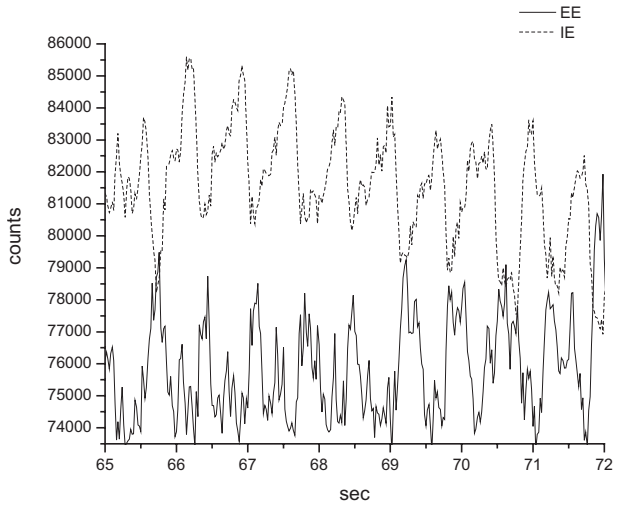

Fig. 3 Same data as in Fig. 2, shown at higher temporal resolution to show complementary behavior of elastically scattered light (EE) versus inelastically produced light (IE).

tum corneum. The EE region contains only reflected and elastically scattered light.

To initiate a measurement sequence, a fingertip is brought into contact with a spring steel surface having a 2-mm-diam hole through which a 100-μm-diam laser beam contacts the fingertip. The pressure at this point is 20 ± 5 g/cm^2 and is almost imperceptible to test subjects. Collection of CCD frames is initiated on application of a very short and weak mechanical impulse applied to the back of the fingertip, contacting between the upper joint and cuticle with the end of a rounded smooth Teflon® cylinder 5 mm in diameter. The pressure goes from $\approx$20 to $\approx$50 g/cm^2 in 0.1 s. Direct observation of the skin surface through the optical system during the entire process shows that the laser spot moves <10 μm throughout. The apparatus allows the applied force and contact area to be continuously monitored, so that the pressure between the fingertip and the spring steel surface is actively maintained. Depending on the turgor of the particular test subject, the tissue flattens and the contact area increases throughout the experiment thus requiring an increase in force to continuously meet the pressure set point.

The observations are for virtually every person we observed. Subjects were from age 8 to 80, with many skin tones and ethnicities, healthy, diseased, and of both sexes. Different test subjects require different pressure conditions to properly balance the blood and oncotic pressures. An applied pressure between the diastolic and systolic blood pressures is a good starting point for finding optimal conditions.

3 Results and Discussion

Figure 2 shows typical data corresponding to the sequence described above. The IE and EE integrals are each plotted as a function of time. The data were transformed to have a mean of 0 and standard deviation of 1 to facilitate their comparison. In the inset, we show the data for $t<0.5$ s. Initially, the IE drops rapidly while the EE is nearly constant. Figure 3 shows some of the same data as Fig. 2 but using an expanded temporal scale to show the complementary and very nearly proportional behavior of EE versus IE light.

The heart-driven pulses are obvious and can be easily confirmed as such using a common commercial blood pressure/pulse rate cuff and by doing experiments that change the test subject's pulse rate (i.e., physical exertion or execution of the Valsalva maneuver). Although we shall not concern ourselves with them here, there are regular, longer time-scale fluctuations observable in Fig. 2 that are reproducible and at least partially due to known correlations between the pulse and breathing rhythms.

To understand the relative time dependence of the EE and IE data on the time scale of the pulses and faster, two facts are important. First, we previously published *in vitro* data for 785-nm excitation of methemoglobin (Hb) over the concentration range spanning the normal capillary blood range, demonstrating that the integrated fluorescence (i.e. IE) increases linearly[12] with increasing hemoglobin volume percent. At higher concentrations there is significant photobleaching. We recently measured the analogous dependence for *in vitro* plasma fluorescence, and it also increases linearly from infinite dilution in Normocarb™ to pure plasma. Thus, fluorescence measured *in vivo* is a measure of both plasma volume and hemoglobin volume.

Second, the amount of elastically scattered light collected decreases as the volume percent of RBCs increases. In perfused skin, the volume percentages of the plasma, RBC, and static tissues are constantly changing. A volume containing only static tissue and plasma would not scatter appreciably because the scattering coefficients are small. But propagation through a perfused volume may experience much larger changes because of changed RBC volume fraction, because RBC scattering coefficients are very large. If, for a heart-driven pressure wave (i.e. pulse) the volume percentage of plasma decreases, the volume percent of RBCs must increase, even if none actually moved, and the net elastically scattered light collected will decrease.

Thus, at the shortest times, when the actuator is establishing control over the pressure applied to the tissue, the behavior of the two plots (substantial decrease in IE with a *small* relative change in the EE) suggests that mostly plasma motion occurs. Because plasma motion out of the irradiated volume *increases* the RBC volume percent and causes a decrease in elastically scattered light collected, we infer that the observed change in IE is due mostly to plasma removal. Apparently the small observed change in EE signal is due to a small movement of RBCs out of the irradiated volume, which keeps the change in volume percent of RBCs in the irradiated volume very small. This seems reasonable because, in the depth range we observe in Fig. 2 plasma and erythrocytes are mostly confined to narrow capillaries and the discharge and tube hematocrit[13] are very nearly equal. The effect of a relatively large change in IE due to plasma motion is compensated by a very small modulation of RBCs so the RBC volume fraction is nearly constant.

Once the desired pressure value has been established, the pulses and other regular temporal oscillations in both the IE and EE data can be observed. The IE temporal behavior corresponds to the increasing and decreasing local blood volume as blood pressure pulses propagate through the capillaries in the irradiated volume. The capillaries become slightly distended as an increased volume of plasma and RBCs occupies the capillary lumen during the increasing pressure pulse. Because the RBCs have by far the largest scattering coefficient, change of EE *collected* light is most strongly associated with RBC movement. Although most of the observed Rayleigh/Mie light originates from static tissue because that tissue has the highest volume fraction, the efficiency of *propagation* of the excitation light to the static tissue and of the elastically scattered light to the collection zone decreases as RBC volume percent increases.

We will soon publish a model for the propagation and scattering of radiation through skin based on radiative transfer theory, that includes the attenuation of incoming radiation by scattering and absorption, the scattering of the radiation from all tissues and the propagation of scattered radiation from scattering centers to the detector. Calculations based on the model successfully predict the optimum values for geometrical and other parameters of the apparatus. Using the optical parameters given above and assumed values for volume fractions, it accounts for the observed effects and gives their interpretation. There are two *independent* measurements, the IE, associated with the combined plasma and RBC volume fractions, and the EE, associated exclusively with the RBC volume fraction. By fitting results for the fingertip capillaries to our model with the two volume fractions as parameters, we can obtain a quantitative measure of hematocrit noninvasively.

4 Conclusions

Simultaneous observation of elastic scattering, fluorescence, and inelastic scattering from *in vivo* NIR probing of human skin allows discrimination of the movement and presence of RBCs independently from plasma. Control of the mechanical force needed to obtain reliable optical registration of *in vivo* tissue with our optical system allows reproducible observation of blood flow in capillary beds of human volar side fingertips. The time dependence of the elastically scattered light is complementary to that of the combined fluorescence and Raman scattered light due to the changing volume fractions of the tissues in the irradiated volume with normal homeostatic processes (i.e., heart-driven pulses) and the impeding effect of red blood cells on optical propagation.

Acknowledgments

This research was supported by LighTouch Medical. We appreciate the continued collaboration of Lou Buda, Charlie Brown, Phil Arnold, Les Schmutzler, Richard Steinmann, R. Acevedo, and William Finney, as well as Dave Stehlik, Dan Godici, John Fayos, and Dave Rice of Critical Link LLC.

References

1. V. Tuchin, *Tissue Optics*, SPIE Press, Bellingham (2000).
2. J. Chaiken, W. F. Finney, K. Peterson, C. M. Peterson, P. E. Knudson, R. S. Weinstock, and P. Lein, "Noninvasive, *in vivo*, tissue modulated near infrared vibrational spectroscopic study of mobile and static tissues: blood chemistry," *Proc. SPIE* **3918**, 135–143 (2000).
3. J. Chaiken, W. F. Finney, P. E. Knudson, K. Peterson, C. M. Peterson, R. J. Bussjager, Y. Zhao, R. S. Weinstock, M. Khan, D. Hagrman, and P. Hagrman, "The effect of hemoglobin concentration variation on the accuracy and precision of glucose analysis using tissue modulated, noninvasive, *in vivo* Raman spectroscopy of human blood: a small clinical study," *J. Biomed. Opt.* **10**, 031111 (2005).
4. J. Chaiken, K. Ellis, P. Eslick, L. Piacente, and E. Voss, "Noninvasive *in vivo* tissue and pulse modulated Raman spectroscopy of human capillary blood and plasma," *Proc. SPIE* **6093**, 609305 (2006).
5. E. Salamotino, B. Jiang, J. Novak, and A. N. Yaroslavsky, "Optical properties of normal and cancerous human skin in the visible and near infrared spectral range," *J. Biomed. Opt.* **11**(6), 064026 (Nov./Dec. 2006).
6. S. L. Jacques, "Origins of tissue optical properties in the UVA, Visible, and NIR regions," in *OSA TOPS on Advances in Optical Imaging and Photon Migration*, R. R. Alfano, and J. G. Fujimoto, Eds., Vol. **2**, pp. 364–369, Optical Society of America, Washington, DC (1996).
7. M. Meinke, G. Muller, J. Helfmann, and M. Friebel, "Optical properties of platelets and blood plasma and their influence of the optical behavior of whole blood in the visible and near infrared wavelength range," *J. Biomed. Opt.* **12**(1), 014024 (2007).
8. S. Singh and R. A. Swerlick, "Dermal Blood Vessels," American Academy of Dermatology, http://www.aad.org/education/students/DermalBloods.htm.
9. P. Williams, Ed., *Gray's Anatomy*, 38th ed., p. 1465, Churchill Livingston, New York (1999).
10. C. Lentner, Ed., *Geigy Tables*, 8th ed., Vol. **5**, p. 545, CIBA-Geigy, Basel (1990).
11. J. Chaiken, E. Voss, Rebecca J. Bussjager, and G. Shaheen, "Towards an improved assignment of spectral features in tissue modulated noninvasive Raman spectroscopy of human fingertips," *Proc. SPIE* **6430**, 643004 (2007).
12. J. Chaiken, W. F. Finney, X. Yang, P. E. Knudson, K. Peterson, C. M. Peterson, R. S. Weinstock, D. Hagerman, "Progress in the noninvasive, *in vivo*, tissue modulated Raman spectroscopy of human blood," *Proc. SPIE* **4254**, 216–227 (2001).
13. C. D. Forbes and G. D. O. Lowe, in *Physics in Medicine and Biology Encyclopedia*, T. F. McAnish, Ed., Vol. **1**, p. 105, Pergammon Press, New York (1986).